Proceedings of the ASME 2022 41st International Conference on Ocean, Offshore and Arctic Engineering
OMAE2022
June 5-10, 2022, Hamburg, Germany

OMAE2022-78643

IMPORTANCE OF THE INERTIAL COMPONENTS IN MODAL STATE COVARIANCES

Margaux Geuzaine
Structural and Stochastic Dynamics
UEE Department, University of Liège
Liège, Belgium

Aksel Fenerci
Ocean Applications and Civil Engineering Dept.
Norwegian University of Science and Technology
Ålesund, Norway

Ole Øiseth
Department of Structural Engineering
Norwegian University of Science and Technology
Trondheim, Norway

Vincent Denoël
Structural and Stochastic Dynamics
UEE Department, University of Liège
Liège, Belgium

ABSTRACT

The modal state responses of very large floating structures subjected to sea waves are addressed in this paper. Semi-analytical approximations for their second order statistics are first provided. They are derived by using the multiple timescale spectral analysis and they aim at calculating the variances of the nodal state responses much more rapidly than with the traditional time and frequency domain methods. Based on these approximate formulas, such expressions are developed for the correlation coefficients in this paper. They allow to understand in which cases the covariances between two modal state responses are significant and cannot legitimately be neglected. They are for instance important to consider when the natural frequencies of the corresponding modes are close to one another or when their shapes are similar. The accuracy of the proposed expressions is then verified on a realistic example inspired by an actual floating pontoon bridge. The results are shown to be less precise, although still acceptable, when the peak frequency of the loading and the natural frequencies of the structure are of the same order of magnitude. This is to be expected since the validity of the proposed approximations is conditioned upon the separation of these timescales.

Keywords: multiple timescale spectral analysis, inertial loading, modal covariances, state formulation, correlation coefficients.

NOMENCLATURE

Lowercase and capital bold letters are respectively used for denoting vectors and matrices. Italic letters are employed for their elements. The superscripts $(.)^*$, $(.)^\intercal$, and $(.)^\dagger$ respectively stand for the conjugate, the transpose and the conjugate transpose, or hermitian, operators.

1. INTRODUCTION

In order to cross wide and deep fjords or straits, long-span bridges usually have to be supported by floating supports. However, traditional time and frequency domain analysis methods actually struggle to evaluate the extreme response to the hydrodynamic actions of such large floating structures in a reasonable amount of time because the timescales associated with the motions of either the structure, either the loading, are most often clearly separated.

Indeed, in the time domain, it relies on the statistical treatment of response signals. Unfortunately, they have to be simulated long enough to capture the slow dynamics of the floaters, and with a sufficiently short time step to capture the fast dynamics of the waves. Similarly, in the frequency domain, sharp and distant peaks appear in the spectral densities of the responses. Their numerical integration therefore requires using many closely spaced points, spread over a wide domain, to provide a correct estimation of the response statistics which are then used for determining the extreme distribution [1].

Despite being more efficient than the generation of time histories, the computational cost of the analysis in the frequency domain becomes prohibitive as well for large structures with many degrees-of-freedom. Currently, the complexity of this method is driven by the projections of the matrix containing the spectral densities of the forces into the modal basis. It is indeed a time-consuming operation which additionally has to be repeated at each of the numerous integration points along the frequency axis.

This problem is tackled in this paper by deriving semi-analytical approximations for the integrals at stake which allow to drastically reduce the number of modal projections required for computing these integrals with a sufficient accuracy. To do so, the multiple timescale spectral analysis is used. This general framework is based on perturbation theories and is known to provide simple expressions to approximate the statistics of the responses very quickly with a controllable discrepancy. It can actually be seen as a generalization of the background-resonant decomposition which is associated to the variances of the responses experienced by a single degree-of-freedom system under a buffeting wind loading [2].

Until now, the multiple timescale spectral analysis has mainly been applied in a wind engineering context as well [3]–[7]. In this paper, however, such a simple expression is sought for the second order statistics of the modal state responses of wave-loaded structures, the main difference being that they might be excited in their inertial regime as well [8]. This formula is then manipulated to get a similar approximation for the modal correlation coefficients so that it is possible to derive in an analytical way the conditions under which the influence of the modal covariances is significant or not. Illustrations are finally provided for a simplified example inspired by the Bergsøysund Bridge, which is an actual floating pontoon bridge located in Norway.

2. FREQUENCY DOMAIN SPECTRAL ANALYSIS

2.1. Deterministic Analysis

The dynamics of a linear elastic structure with N degrees-of-freedom subjected to sea waves is governed by a set of N second order differential equations which reads

$$[\boldsymbol{K} + i\omega\boldsymbol{C} - \omega^2\boldsymbol{M}]\boldsymbol{x}(\omega) = \boldsymbol{f}(\omega) \tag{1}$$

where i is the imaginary unit, ω is the circular frequency, $\boldsymbol{x}(\omega)$ and $\boldsymbol{f}(\omega)$ are two $N \times 1$ vectors containing the frequency-domain representations of the structural displacements in every degree-of-freedom and the undisturbed wave loads acting on each of them, respectively, while $\boldsymbol{K}$, $\boldsymbol{C}$, and $\boldsymbol{M}$, denote the sum of the structural and hydrodynamic stiffness, damping and mass matrices.

Being related to fluid-structure interactions, the latter three matrices should in principle depend on the frequency but this particularity is discarded in the present paper, for the sake of simplicity. Instead, the frequency sensitivity of these matrices is considered limited enough to be neglected. Their elements are thus replaced by their values at ω_0 being the predominant frequency of the forces or of the motions [9]–[11].

Unfortunately, the hydrodynamic damping is typically neither classical [12], nor negligible [11], and it is necessary to rewrite Equation (1) in terms of the state responses and the state forces, $\boldsymbol{y}(\omega) = [\boldsymbol{I} \quad i\omega\boldsymbol{I}]^\intercal\boldsymbol{x}(\omega)$ and $\boldsymbol{g}(\omega) = [\boldsymbol{I} \quad 0]^\intercal\boldsymbol{f}(\omega)$ where I and 0 are respectively an identity and a zero $N \times N$ matrix, as

$$[\boldsymbol{A} + i\omega\boldsymbol{B}]\boldsymbol{y}(\omega) = \boldsymbol{g}(\omega) \tag{2}$$

in order to find an appropriate basis of size $2N \times 2M$ with 2M $\ll$ 2N which is simultaneously able to decouple the equations and to reduce drastically their number, even though the state matrices

$$\boldsymbol{A} = \begin{pmatrix} \boldsymbol{K} & \boldsymbol{0} \\ \boldsymbol{0} & -\boldsymbol{M} \end{pmatrix} \quad \& \quad \boldsymbol{B} = \begin{pmatrix} \boldsymbol{C} & \boldsymbol{M} \\ \boldsymbol{M} & \boldsymbol{0} \end{pmatrix} \tag{3}$$

are twice as large as the initial matrices $\boldsymbol{K}$, $\boldsymbol{C}$, and $\boldsymbol{M}$ [13], [14].

The matrix $\boldsymbol{\Theta}$ usually gathers the shapes of the 2M most contributing modes. They are obtained as the solutions of the complex eigenvalue problem associated to the homogeneous part of the governing equations

$$i\boldsymbol{A}\boldsymbol{\Theta} = \boldsymbol{B}\boldsymbol{\Theta}\boldsymbol{\Lambda} \tag{4}$$

together with the diagonal matrix $\boldsymbol{\Lambda}$ which collects the corresponding eigenvalues

$$\lambda_m = \psi_m + i\upsilon_m \text{ with } \begin{cases} \psi_m = (-1)^m\sqrt{1-\xi_{j_m}^2}\,\omega_{j_m} \\ \upsilon_m = \xi_{j_m}\omega_{j_m} \quad , \quad j_m = \left\lceil \frac{m}{2} \right\rceil \end{cases} \tag{5}$$

where ω_{j_m} and ξ_{j_m} are the j-th natural frequency and damping ratio of the undamped wet structure.

The modal projection and decomposition of the state forces and responses, $\boldsymbol{y}(\omega) = \boldsymbol{\Theta}^\intercal\boldsymbol{q}(\omega)$ and $\boldsymbol{p}(\omega) = \boldsymbol{\Theta}^\intercal\boldsymbol{g}(\omega)$, are then introduced into Equation (2). This equation is subsequently left-multiplied by $\boldsymbol{\Theta}^\intercal$ to give

$$q_m(\omega) = D_m H_m(\omega) p_m(\omega) \tag{6}$$

where D_m is a normalization constant ensuring that the real or the imaginary parts of the m-th mode reach one at most in absolute value, depending on whether m is odd or even, and

$$H_m(\omega) = (\lambda_m - \omega)^{-1} \tag{7}$$

is the m-th frequency response function. On top of being scalar, it also contains a single pole. The modal state responses are therefore monochromatic, in addition to being decoupled.

2.2. Stochastic Analysis

When dealing with deep water waves of moderate height [11], the hydrodynamic forces can be considered as being Gaussian. So are therefore the responses given that the structure is also linear. These processes are also zero-mean because they are defined with respect to the static equilibrium configuration.

In this event, both the forces and the responses are fully characterized, in a probabilistic sense, on the sole basis of their power spectral densities. In particular, their probability density function is completely defined once their variance is established.

Thanks to the state formulation and the modal decomposition, the probabilistic properties of the nodal state responses can be efficiently computed based on those of the forces, which are supposed to be known. The cross-spectral density of the i-th and j-th nodal state responses, for instance, is given as

$$S_{y,ij}(\omega) = \sum_{m=1}^{2M}\sum_{n=1}^{2M} \Theta_{im}\Theta_{jn}^* S_{q,mn}(\omega) \tag{8}$$

by combining linearly the cross-spectral densities of the m-th and n-th modal state responses which read as follows

$$S_{q,mn}(\omega) = D_m D_n G_{mn}(\omega) S_{p,mn}(\omega) \tag{9}$$

where

$$G_{mn}(\omega) = H_m(\omega) H_n^*(\omega) \tag{10}$$

is the (m,n)-th structural kernel and

$$S_{p,mn}(\omega) = \sum_{i=1}^{N} \sum_{j=1}^{N} \Theta_{im} \Theta_{jn}^* S_{f,ij}(\omega) \tag{11}$$

is the cross-spectral density of the m-th and n-th modal state forces.

The projection performed in Equation (11) is currently the most time-consuming operation of the analysis. Unfortunately, it has to be repeated at a large number of closely spaced frequencies in order to determine the covariances of the modal state responses

$$\Sigma_{q,mn} = \int_{-\infty}^{+\infty} S_{q,mn}(\omega) d\omega \tag{12}$$

and thus the variances of the nodal state responses

$$\Sigma_{y,ii} = \sum_{m=1}^{2M} \sum_{n=1}^{2M} \Theta_{im} \Theta_{in}^* \Sigma_{q,mn} \tag{13}$$

with a sufficient accuracy. The closeness of these integration points is required because the function to be integrated features up to two sharp peaks, at most, which are respectively associated to the resonance of the structure in the m-th and the n-th modes. Moreover, the integrand also exhibits some strong variations related to the particular energy content of the waves.

3. MULTIPLE TIMESCALE SPECTRAL ANALYSIS

3.1. Method Summary

Fortunately enough, the peaks associated to the resonance of the structure are most often very well separated from the peaks that are coming from the cross-spectral densities of the loading. The multiple timescale spectral analysis is a general framework dedicated to the derivation of semi-analytical approximations for integrating such functions with distinct peaks. They are known to drastically reduce the number of integration points that are required and thus the number of frequencies at which the cross-spectral densities of the loading are computed and projected.

In the present configuration [15], the separation of the peaks in the cross-spectral density of the m-th and n-th modal state responses is conditioned upon the following assumptions:

(i) The cross-spectral density of the m-th and n-th modal state forces is varying smoothly and moderately over the width of the resonant peaks. In other words, the derivatives of this cross-spectrum are considered small enough to maintain the asymptoticness of its Taylor series expansion in the neighborhood of these peaks, near ψ_m and ψ_n, with respect to their extent. More formally, it reads

$$(\omega - \psi_m)^i \partial_\omega^i S_{p,mn}(\psi_m) \ll S_{p,mn}(\psi_m) \tag{14}$$

and

$$(\omega - \psi_n)^i \partial_\omega^i S_{p,mn}(\psi_n) \ll S_{p,mn}(\psi_n) \tag{15}$$

where ∂_ω^i represents the i-th circular frequency derivative.

(ii) The characteristic frequency of the loading, which is denoted ω_p, is significantly different from the m-th and n-th natural frequencies of the structure, ψ_m and ψ_n. This is formalized by noticing that the frequency ratios

$$\alpha_m = \frac{\omega_p}{|\psi_m|} \quad \& \quad \alpha_n = \frac{\omega_p}{|\psi_n|} \tag{16}$$

are either much lower, either much greater than one.

In these circumstances, it is possible to demonstrate, see details in [15], that the covariance of the m-th and n-th modal state responses can approximately be decomposed into two main components as follows

$$\tilde{\Sigma}_{q,mn} = \Sigma_{r,mn} + \Sigma_{\ell,mn}. \tag{17}$$

The first term is due to the peaks of the structural kernel and is thus called *resonant*. The second term is coming from the peaks of the loading cross-spectrum and can therefore be named *background* if both $\alpha_m < 1$ and $\alpha_n < 1$, *inertial* if both $\alpha_m > 1$ and $\alpha_n > 1$, or *mixed* otherwise. In general, though, it will be referred to as the *loading* component.

Nevertheless, this second component should drop when one or both natural frequencies are close to the characteristic frequency of the loading. Indeed, the peak of the loading cross-spectrum is stacked on one or both peaks of the structural kernel in this specific event and the resonant component is expected to encompass them all at once.

3.2. Resonant Component

In Equation (17), the resonant component of the modal state covariance reads

$$\Sigma_{r,mn} = i\pi \frac{D_m D_n}{\lambda_m - \lambda_n^*} \left[S_{p,mn}(\psi_m) + S_{p,mn}(\psi_n) \right] \tag{18}$$

and corresponds to the integral of

$$S_{r,mn}(\omega) = -\frac{D_m D_n}{\lambda_m - \lambda_n^*} \left[H_m(\omega) S_{p,mn}(\psi_m) - H_n^*(\omega) S_{p,mn}(\psi_n) \right] \tag{19}$$

which approximates locally the cross-spectral density of the m-th and n-th modal state responses over their resonant peaks. It was obtained by expanding the structural kernel in partial fraction, first, to get a sum of two rational functions with single poles.

The integrand was thus separated into two parts, each of them with their own resonant peak, across which the multiplying

cross-spectral density of the m-th and n-th modal state forces was then replaced by the constant values $S_{p,mn}(\psi_m)$ and $S_{p,mn}(\psi_n)$ respectively.

3.3. Loading Component

The loading component is more involved, mathematically speaking, because it covers three different cases. Nevertheless, its behavior regarding some modifications of the input parameters is overall simple to understand. Indeed, it reads

$$\begin{aligned}\Sigma_{\ell,mn} &= D_m D_n L_{mn}\left(\sum_{k=1}^{4}\left(+\omega_p\right)^{\beta_k}\mathcal{G}_{mn}^{(k)}\left(+\omega_p\right)\Sigma_{p,mn}^{(k)(+)}\right. \\ &\left.+\sum_{k=1}^{4}\left(-\omega_p\right)^{\beta_k}\mathcal{G}_{mn}^{(k)}\left(-\omega_p\right)\Sigma_{p,mn}^{(k)(-)}\right)\end{aligned} \tag{20}$$

where

$$\Sigma_{p,mn}^{(k)(\pm)} = \pm\int_{0}^{\pm\infty}\omega^{-\beta_k}S_{p,mn}(\omega)d\omega \tag{21}$$

can be seen as a part of $(-\beta_k)$ spectral moment associated to the corresponding modal state forces and the multiplicative factor

$$L_{mn} = \left(1-\frac{S_{p,mn}(\psi_m)}{S_{p,mn}(\omega_p)}\right)\left(1-\frac{S_{p,mn}(\psi_n)}{S_{p,mn}(\omega_p)}\right) \tag{22}$$

forces the loading component to drop down to zero as it should when the multiple timescale spectral analysis does not provide valid expressions anymore, e.g. when the frequency ratios are close to one, or when the modal covariance is just fully resonant, e.g. the cross-spectral density of the modal state forces does not feature any peak. The function $\mathcal{G}_{mn}^{(k)}(\pm\omega_p)$ and the exponent β_k, for their part, are listed for all k indices in Table 1 where

$$\beta_{m,n} = \left((-1)^{m,n}\alpha_{m,n}^{-1}-1\right)^{-1} \tag{23}$$

is given by 0 or 1 at leading order if $\alpha_{m,n} \ll 1$ or $\alpha_{m,n} \gg 1$. Their definitions are resulting from the replacement of the real and the imaginary parts of the frequency response functions over the positive or the negative frequency range by a monomial which is equal to the initial function at the location of the loading peak occurring in the considered frequency range and which is characterized by the same slope in logarithmic scales.

TABLE 1: DEFINITIONS FOR EQUATIONS (20) AND (24)

k	β_k	$\mathcal{G}_{mn}^{(k)}(.)$
1	$\beta_m+\beta_n$	$\Re H_m(.)\Re H_n^*(.)$
2	$\beta_m+2\beta_n$	$i\Re H_m(.)\Im H_n^*(.)$
3	$2\beta_m+\beta_n$	$i\Im H_m(.)\Re H_n^*(.)$
4	$2\beta_m+2\beta_n$	$-\Im H_m(.)\Im H_n^*(.)$

Similarly to before, the loading component presented in Equation (20) corresponds to the integral of

$$\begin{aligned}&\mathcal{S}_{\ell,mn}^{(\pm)}(\omega) \\ &= D_m D_n L_{mn}\sum_{k=1}^{4}\left(\pm\omega_p\right)^{\beta_k}\mathcal{G}_{mn}^{(k)}\left(\pm\omega_p\right)\mathcal{S}_{p,mn}^{(k)(\pm)}(\omega)\end{aligned} \tag{24}$$

which is the local approximation derived for the cross-spectral density of the m-th and n-th modal state responses over the loading peaks. Given its non-symmetric nature, the symbols $(+)$ and $(-)$ have to be selected in accordance with the sign of the circular frequency.

3.4. Relative Importance

Based on the simple formulae established in the previous sub-sections, it is possible to derive similar expressions for the correlation coefficients. Being dimensionless, they allow to assess the importance of modal covariances when computing the nodal responses. The correlation coefficients can be written like the modal covariances as the sum of a resonant and a loading component:

$$\rho_{q,mn} = \gamma_r\rho_{r,mn} + \gamma_\ell\rho_{\ell,mn} \tag{25}$$

where

$$\gamma_r = \frac{1}{\sqrt{1+r_m^{-1}}\sqrt{1+r_n^{-1}}} \;\;\&\;\; \gamma_\ell = \frac{1}{\sqrt{1+r_m}\sqrt{1+r_n}} \tag{26}$$

can be seen as weighting factors. They are related to the resonant-to-loading ratios of the corresponding modal variances as follows

$$r_m = \frac{\Sigma_{r,mm}}{\Sigma_{\ell,mm}} \quad\&\quad r_n = \frac{\Sigma_{r,nn}}{\Sigma_{\ell,nn}} \tag{27}$$

and accordingly tend toward unity or zero if the modal responses are predominantly driven by their resonant or loading components, e.g. $\gamma_r = 1$ and. $\gamma_\ell = 0$ if both $r_m \gg 1$ and $r_n \gg 1$, meaning that the responses are fully resonant.

Substituting the appropriate components of the modal variances and covariances given by Equation (18) and Equation (20) in the following expression

$$\rho_{(.),mn} = \frac{\Sigma_{(.),mn}}{\sqrt{\Sigma_{(.),mm}\Sigma_{(.),,nn}}} \tag{28}$$

yields the resonant and the loading coefficients. The former interestingly reads

$$\rho_{r,mn} = i\frac{\sqrt{\upsilon_m\upsilon_n}}{\lambda_m-\lambda_n^*}\left[\Gamma_{mn}(\psi_m)S_{mn}+\Gamma_{mn}(\psi_n)S_{nm}\right] \tag{29}$$

which increases if the natural frequencies are getting closer to one another and if the values of the coherence function

$$\Gamma_{mn}(\omega) = \frac{S_{p,mn}(\omega)}{\sqrt{S_{p,mm}(\omega)S_{p,nn}(\omega)}} \tag{30}$$

at $\omega = \psi_m$ and $\omega = \psi_n$ comprised within the $[-1;1]$ interval grow as well, together with the spectral ratios

$$S_{mn} = \sqrt{\frac{S_{p,nn}(\psi_m)}{S_{p,nn}(\psi_m)}} \quad \& \quad S_{nm} = \sqrt{\frac{S_{p,mm}(\psi_n)}{S_{p,mm}(\psi_n)}} \qquad (31)$$

they respectively multiply. The latter coefficient, however, is not easily interpretable unless the loading component is quasi-static in both modes, in which case it corresponds to the correlation coefficient of the modal state forces at leading order, i.e. $\rho_{\ell,mn} = \rho_{p,mn}$ if $\alpha_m \ll 1$ and $\alpha_n \ll 1$.

4. EXAMPLE: BERGSØYSUND BRIDGE

4.1. Finite Element and Load Modelling

The proposed formulae are now validated on a simplified 2D model, considering the surge response only, of the Bergsøysund Bridge which crosses a 100 m deep strait in Norway and is one of the longest end-anchored floating bridge in the world with its total length of 933 m. As shown in Figure 1, it is composed of 7 pontoons linked together by steel truss segments of 105 m long, which are just modelled as single equivalent beams with 10 elements of equal length by section for the sake of the illustration in this paper.

Despite being realistic, their properties are given in Table 2 and have been chosen to ensure that the background and the inertial regimes are respectively activated in a few modes by the loading. Some of the resulting natural frequencies and damping ratios are listed in Table 3 while the corresponding mode shapes are represented in Figure 2.

Except for these differences, the pontoons and the forces are defined as in Kvåle's paper [11] with a significant wave height of 2.4 m and a peak frequency of 2.2 rad/s at which the hydrodynamic matrices are evaluated, as explained in Section 2. A spreading parameter of 3 is also selected because it allows to neglect the correlations between the forces applied on different pontoons.

TABLE 2: PROPERTIES OF THE FINITE ELEMENTS

PARAMETER	VALUE
Length	10.5 [m]
Moment of Inertia	12.36 [m^4]
Young Modulus	2.10^{10} [N/m^2]
Cross-Section	0,6 [m^2]
Density	7850 [kg/m^2]

4.2. Results

Figure 3 compares the modal variances computed by means of the proposed approximation, see Eq. (17), to the values obtained through the numerical integration of the response power spectral densities, see Eq. (12) with $m = n$. Overall, they coincide quite well, except in the shaded area where a more important discrepancy is observed but this was to be expected because the assumption (ii) is not verified in this zone. The responses in these modes are actually neither mainly resonant, contrary to what the figure suggest, neither quasi-static, nor inertial. The peaks of the loading and the peaks of the kernel are

TABLE 3: RESULTS OF THE MODAL ANALYSIS

j_m	ω_{j_m} [rad/s]	ξ_{j_m} [%]
1	0.2732	16.5
2	0.4248	10.1
3	0.6877	5.9
4	0.8910	3.6
8	2.7397	2.7
13	5.3378	2.1

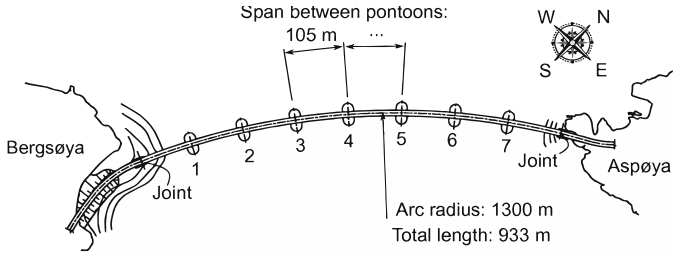

FIGURE 1: TOP VIEW OF THE BERGSØYSUND BRIDGE [11]

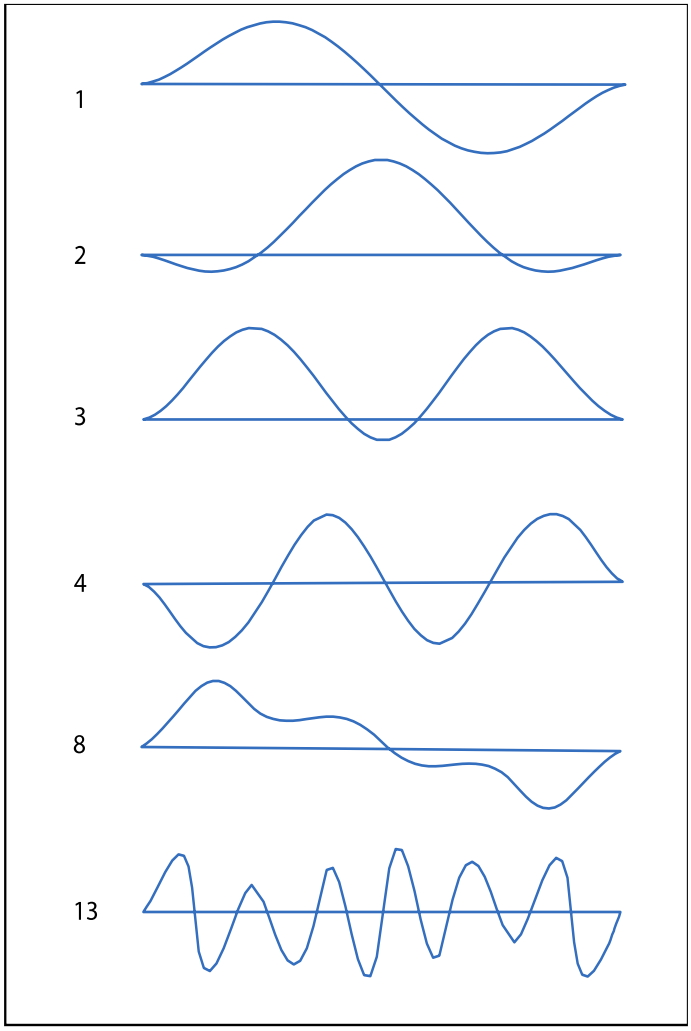

FIGURE 2: MODE SHAPES OF THE 2D MODEL

just interacting. Problem is that larger errors are thus committed on the most contributing components. It might consequently lead to significant differences once the nodal variances are reconstructed. Apart from that, the loading component, see Eq. (20) is clearly leading over the resonant one, see Eq. (18), when the modal responses are activated in their inertial regime. This is due to the exponential decay that the loading cross-spectral densities feature when the frequencies are getting much lower than the peak frequency and that they typically inherit of the wave elevation spectrum. Indeed, if the resonant peaks occur over there, the corresponding component depends on the factor $S_{p,mn}(\psi_m) + S_{p,mn}(\psi_n)$ which is exponentially small.

Figure 4 shows the same results as Figure 3 for the correlation coefficients. They are divided into five categories, and they are referred to as being *partly inertial* in the bottom-left corner, *partly background* in the top-right corner, and *partly mixed* in the two remaining corners, bottom-right and top-left. Meanwhile, the loading and the resonant peaks are interacting again in the middle cross-shaped area. Just as before, a good match is observed, with a bit less accuracy in the central zone, between the approximated and the reference values. The histogram of absolute errors between the results obtained through the proposed approximation and the numerical integration also indicate that most of them are small while their mean value reaches 0.0114 only.

Although the modal correlations are often related to the interaction observed between the resonance in two different modes and neglected provided that their natural frequencies are sufficiently distant from each other as it is confirmed by looking at the resonant components in Figure 4, they also appear to be

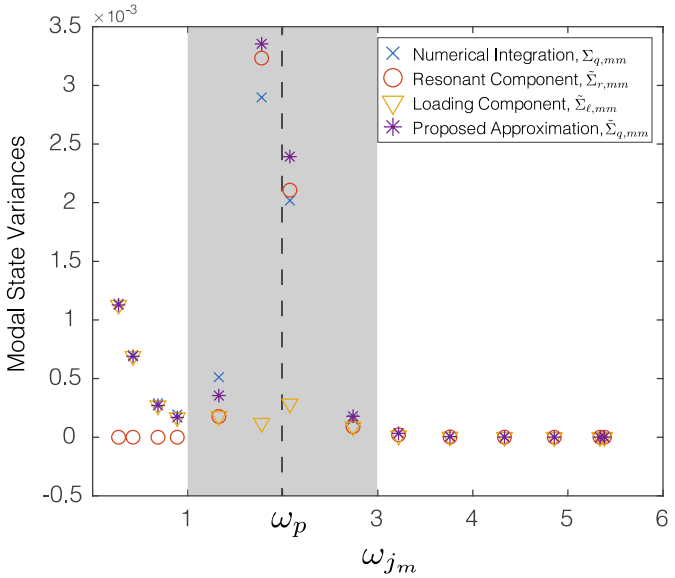

FIGURE 3: MODAL STATE VARIANCES

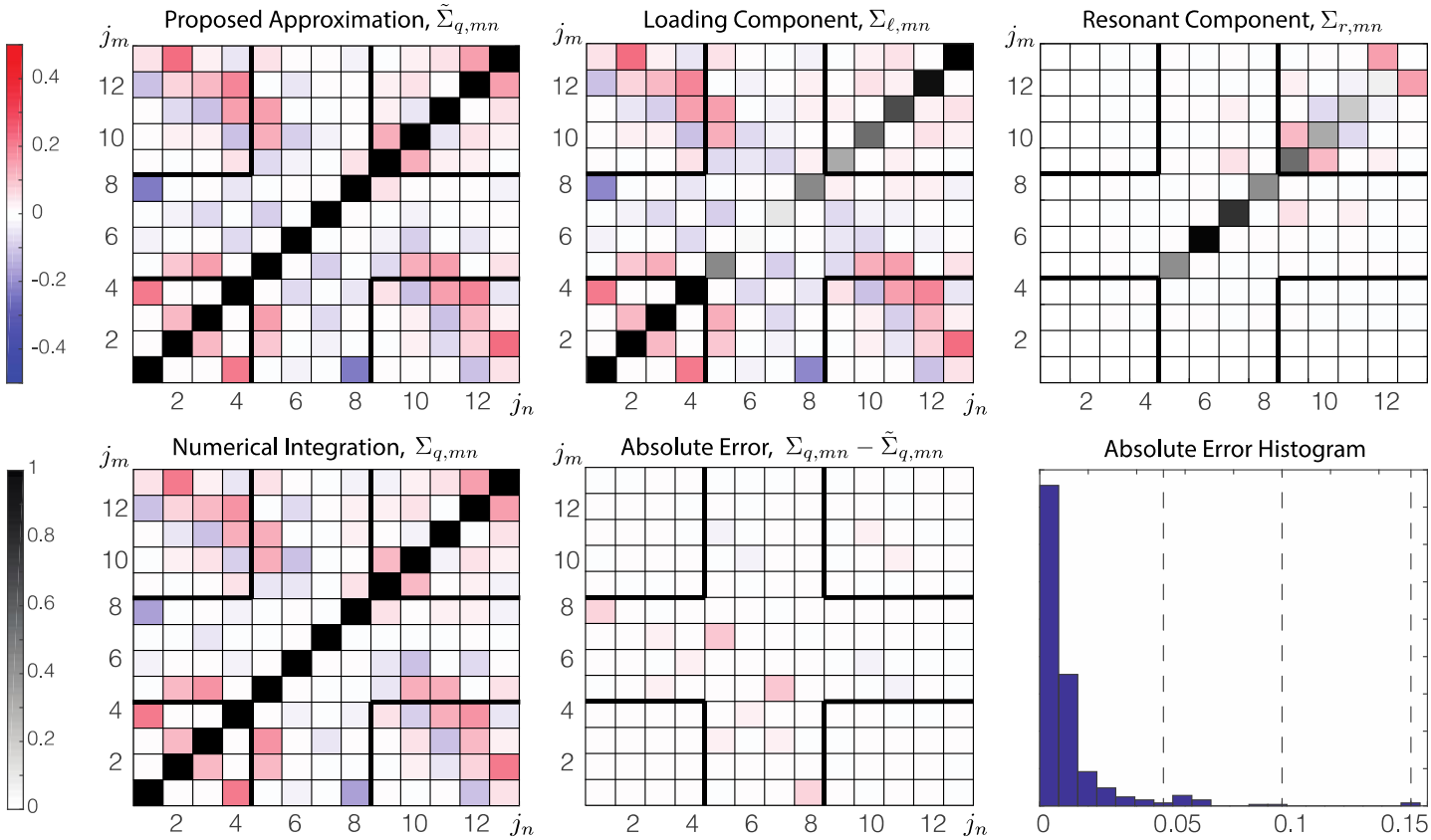

FIGURE 4: REAL PARTS OF THE CORRELATION COEFFICIENTS BETWEEN THE MODAL STATE RESPONSES. THESE COEFFICIENTS ARE DIMENSIONLESS AND COMMONLY DEFINED BY EQ. (28) WHILE THE PROPOSED APPROXIMATION IS GIVEN BY THE SUM OF THE RESONANT AND THE LOADING COMPONENTS, AS INDICATED IN EQ. (26).

significantly influenced by the loading component, which is typically important when the modal forces are coherent. This is usually the case if their respective mode shapes are similar. The 1st and 8th modes, for instance, are both symmetric, changing sign at mid-length and possessing two half waves.

5. CONCLUSION

The multiple timescale spectral analysis is implemented in this paper to derive new approximate semi-analytical formulas for computing more efficiently the variances and the covariances of modal state responses. They are expressed as the sum of a resonant and a loading component. It provides a significant computational speed up because the proposed approximation requires to project the spectral densities of the loading at the natural frequencies only in order to determine the resonant components. The loading components, for their parts, depend on four spectral moments of the modal state forces at most. Each of these four results can interestingly be obtained by means of a single projection after having integrated the corresponding spectral densities in the nodal basis.

The simple formulas introduced for the variances and the covariances of the modal state responses are then used to provide such an expression for the correlation coefficients. It highlights the importance of taking the modal covariances into account, not only when the natural frequencies of the corresponding modes are close to one another, but also when the corresponding modal forces are coherent.

The approximations developed in this paper are finally verified on a 2D bridge model subjected to simplified wave loads. Their accuracy decreases as expected when the assumptions hidden behind the use of the multiple timescale spectral analysis are not respected, for instance if the peak frequency of the loading is getting close to a natural frequency of the structure.

ACKNOWLEDGEMENTS

The financial support of a FRIA grant awarded by the F.R.S.-FNRS (the Belgian Fund for Scientific Research) is acknowledged by the first author. Part of this research was also conducted during her stay at NTNU Trondheim which was partially financed by a Research Stay Grant awarded by the Wallonia-Brussels Federation, a District Grant attributed via the Rotary Club of Seraing and a Scientific Mission Grant received from the University of Liège.

REFERENCES

[1] F.-I. G. Giske, B. J. Leira, and O. Øiseth, “Efficient computation of cross-spectral densities in the stochastic modelling of waves and wave loads,” *Appl. Ocean Res.*, vol. 62, pp. 70–88, 2017.

[2] A. G. Davenport, “The spectrum of horizontal gustiness near the ground in high winds,” *Q. J. R. Meteorol. Soc.*, vol. 87, no. 372, pp. 194–211, 1961.

[3] V. Denoël, “Multiple timescale spectral analysis,” *Probabilistic Eng. Mech.*, vol. 39, pp. 69–86, 2015.

[4] V. Denoël, “Estimation of modal correlation coefficients from background and resonant responses,” *Struct. Eng. Mech.*, vol. 32, no. 6, pp. 725–740, 2009.

[5] V. Denoël, “On the background and biresonant components of the random response of single degree-of-freedom systems under non-Gaussian random loading,” *Eng. Struct.*, vol. 33, no. 8, pp. 2271–2283, 2011.

[6] V. Denoël and L. Carassale, “Response of an oscillator to a random quadratic velocity-feedback loading,” *J. Wind Eng. Ind. Aerodyn.*, vol. 147, pp. 330–344, 2015.

[7] J. Heremans, A. Mayou, and V. Denoël, “Background/Resonant decomposition of the stochastic torsional flutter response of an aeroelastic oscillator under buffeting loads,” *J. Wind Eng. Ind. Aerodyn.*, vol. 208, no. July, 2021.

[8] M. Geuzaine and V. Denoël, “Efficient estimation of the skewness of the response of a wave-excited oscillator,” *Proc. XI Int. Conf. Struct. Dyn. EURODYN 2020*, pp. 3467–3480, 2020.

[9] R. Taghipour, T. Perez, and T. Moan, “Hybrid frequency-time domain models for dynamic response analysis of marine structures,” *Ocean Eng.*, vol. 35, no. 7, pp. 685–705, 2008.

[10] C. M. Wang and B. T. Wang, *Large Floating Structures*. Springer, 2015.

[11] K. A. Kvåle, R. Sigbjörnsson, and O. Øiseth, “Modelling the stochastic dynamic behaviour of a pontoon bridge: A case study,” *Comput. Struct.*, vol. 165, pp. 123–135, 2016.

[12] A. Ibrahimbegovic and E. L. Wilson, “Simple numerical algorithms for the mode superposition analysis of linear structural systems with non-proportional damping,” *Comput. Struct.*, vol. 33, no. 2, pp. 523–531, 1989.

[13] K. A. Foss, “Co-ordinates which uncouple the equations of motion of a damped linear systems,” *J. Appl. Mech.*, vol. 25, no. May, pp. 361–364, 1967.

[14] F. Tisseur, “Backward error and condition of polynomial eigenvalue problems,” *Linear Algebra Appl.*, vol. 309, no. 1–3, pp. 339–361, 2000.

[15] M. Geuzaine, A. Fenerci, O. Øiseth, V. Denoël, "Multiple timescale spectral analysis of floating structures subjected to hydrodynamic loads”, submitted to Probabilistic Engineering Mechanics.